ELSEVIER

European Journal of Pharmaceutics and Biopharmaceutics 44 (1997) 261–267

European Journal of Pharmaceutics and Biopharmaceutics

Paper

Evaluation of pharmaceutical beam bending tests using double-exposure holographic interferometry

Pasi Raatikainen [a,*], Raimo Silvennoinen [b], Jarkko Ketolainen [a], Pertti Ketolainen [b], Petteri Paronen [a]

[a] *Department of Pharmaceutics, University of Kuopio, Kuopio, Finland*
[b] *Väisälä Laboratory, Department of Physics, University of Joensuu, Joensuu, Finland*

Received 10 October 1996; accepted 22 April 1997

Abstract

Cantilever, three- and four-point bending methods used in the determination of intrinsic elasticity of pharmaceutical powders were evaluated with double-exposure holographic interferometry. Microcrystalline cellulose, dicalcium phosphate dihydrate and α-lactose monohydrate were compressed to rectangular beams and the bending measurements of samples captured on holographic images, which were evaluated by calculating the Young's modulus values for both the upper and lower surfaces of the samples. Several methods were used in the moduli calculations. It was found that the four-point bending method seemed to be best for determining results of the elasticity of soft pharmaceutical powders. The superiority of this method was due to the fact that it resulted in the most homogeneous bending along the beams. The results of the three-point bending method were, however, in good agreement with those of the four-point bending method. On the other hand, the cantilever method was observed to be unsuitable for pharmaceutical powders. Inspection of the holograms revealed that the integrity of α-lactose sample beams was inadequate for moduli evaluation. This would not have been noticed with conventional displacement measurements. © 1997 Elsevier Science B.V.

Keywords: Holographic interferometry; Beam bending; Young's modulus; Pharmaceutical excipients

1. Introduction

Knowledge of the deformation properties of pharmaceutical powders is a very important factor in the research and development of tablets. Young's modulus describes the elastic behaviour of a powder material during and after tablet compaction. The bending tests of compressed rectangular beam specimens of different porosities are widely used in different fields of science to evaluate the elastic properties of materials. These methods provide the possibility to extrapolate Young's modulus values to the zero porosity state and thus describe the intrinsic elasticity of the intact solid material. Although, the preparation of even and homogeneous beams, with sufficiently dense structure and wide porosity range, is difficult with some materials [1], this technique has been used successfully for obtaining a numerical parameter describing the elasticity of pharmaceutical powders [2,3].

In this study, three different beam bending tests were evaluated. Double-exposure holographic interferometry was used as the measurement technique [4–6]. The method has been used previously, e.g. in the evaluation of materials used in dentistry, tablet relaxation and cantilever beam bending of pharmaceutical powder compacts [7,8,1]. The elastic behaviour of microcrys-

* Corresponding author. Department of Pharmaceutics, University of Kuopio, P.O. Box 1627, 70211 Kuopio, Finland. Tel.: + 358 71 162494; fax: + 358 71 162456; e-mail: praatika@messi.uku.fi

PII S0939-6411(97)00135-5

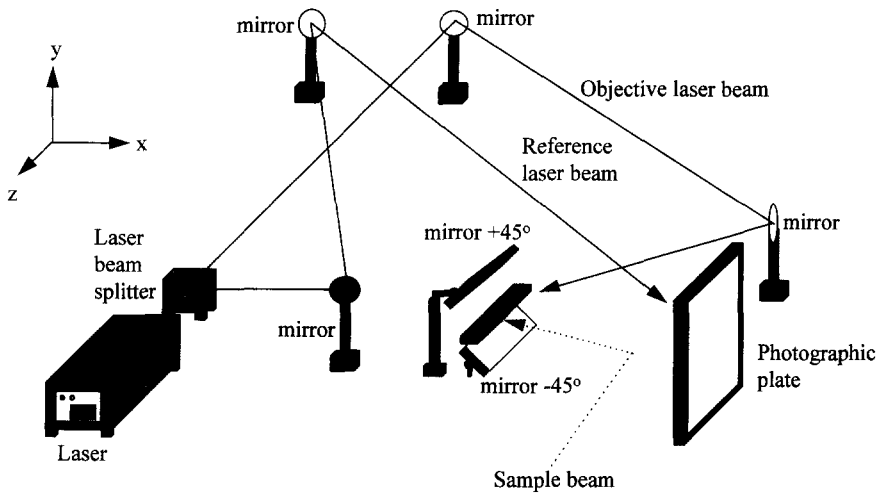

Fig. 1. Double-exposure holographic measurement set-up.

talline cellulose, dicalcium phosphate dihydrate and α-lactose monohydrate were each evaluated by compressing the materials to rectangular beams, and bending the beams with the cantilever, three- and four-point bending methods. The integrity of the beams was also evaluated from the holograms.

2. Materials and methods

2.1. Preparation of samples

The materials tested, microcrystalline cellulose; Avicel® PH-101 (FMC), dicalcium phosphate dihydrate; Emcompress®, (E. Mendell), and α-lactose monohydrate (sieve fraction 149–210 μm); (DMV, Holland), were stored for 2 weeks prior to compression under 45% relative humidity (RH), and the compressed samples were stored for 5 days under the same conditions before the measurement. The rectangular beams, with cross section of 60 × 6 × 2 mm, were compressed using a hardened steel punch and die set and a hydraulic press. The thickness of the beams was adjusted using rejector plates, which stopped the punch from penetrating into the die, providing a sample thickness of 2.0 ± 0.1 mm. Beams with different porosities were prepared by varying the weight of the powder in the die. Ejection of the beam was performed by careful triaxial loosening of the die-set around the compressed beam to avoid inducing any possible structural failure.

2.2. Double-exposure holographic measurement set-up

A schematic view of the double-exposure holographic interferometric measurement is presented in Fig. 1. A ruby laser (JK Lasers 2000, UK) with a wavelength of 694 nm, pulse energy of 1.2 J and pulse duration of the order of 10 ns was used. The laser beam was split in two parts, namely the reference and the object laser beams. The reference laser beam impinged via mirrors directly on to the Agfa Gevaert 10 E 75 (Germany) photographic plate, whereas the object laser beam was directed via mirrors onto the sample surface, from where it was scattered to the photographic plate. The directions of the reference and the scattered laser beams were perpendicular to the sample beam set-ups.

Fig. 2 presents a front view of the sample beam alignment in the different bending methods. In the cantilever beam bending, a sample beam was fixed at one end to a stand with a clamp. The clamp covering a distance of 10 mm at the fixed end of the beam,

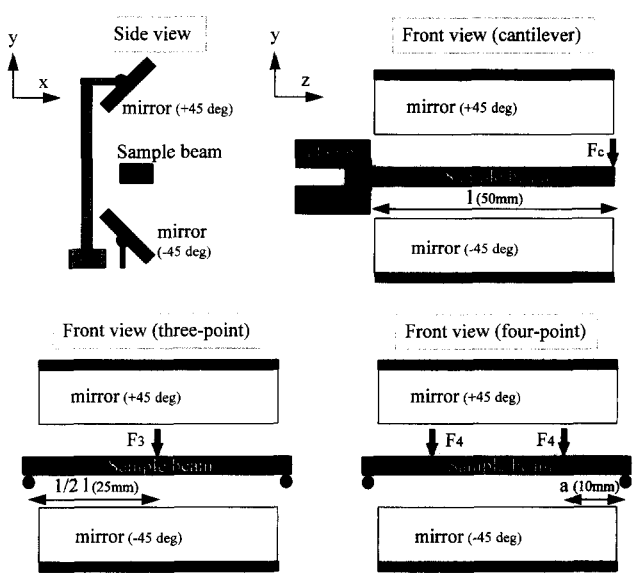

Fig. 2. Side view of the sample beam and mirror alignments, and front views of different bending method set-ups. *l* is the beam length under bending, F_c, *F3* and *F4* are the places at which the bending forces were attached in the cantilever, three- and four point-bending, respectively, and *a* is the span distance in the four-point bending.

produced a constant pressure of 63.8 kPa perpendicular to the beam surfaces under test. The bending force was placed at the free end of the beam. With three- and four-point bending, the sample beam rested freely on the rig. The bending force was directed in the three-point bending method to the middle of the beam under bending, and in the four-point bending method, at both sides 15 mm from the mid-point symmetrically. Bending forces for the first exposures were 0.0207 N for cantilever and 0.1058 N for three- and four-point bending methods, and 0.00311 and 0.00794 N for the second exposures, respectively. An appropriate number of fringes was obtained using these forces. A higher load would have led to problems in the interpretation of the fringes due to lack of contrast between two adjacent fringes, and a lower load would have caused difficulties in the interpretation of bending. The measured part of the beams was 50 mm, and the direction of compression during beam preparation was always noted with all the bending methods. The optical set-up for the double-exposure holographic interferometry was arranged in such a way, that the images of the upper and lower surfaces of the sample beam were recorded simultaneously.

2.3. Recording and reconstruction of holographic images

Double-exposure holographic measurement is based on recording of two separate exposures onto the same photographic plate. Since both exposures appear in coherent light, and exist at approximately the same location in 3-dimensional space, they interfere with each other and produce fringes overlaying the reconstructed hologram. The disturbance causing the interference was generated as the above mentioned weights bent the beam between two separate exposures. When a reconstructed double-exposure hologram was inspected with laser light, two overlapping wavefronts were formed resulting in a typical fringe pattern corresponding to the exposures before and after addition of the weight. The reconstructed images were viewed on a monitor via an image processing system, which consisted of a PC-computer, a gray level framegrabber and a CCD camera. By adjusting the camera position (i.e. the direction of viewing), the holographic images were captured, and the fringe positions on the images of the sample beams (i.e. as they existed along the sample beam length) were marked using the computer's mouse and stored for further evaluation.

2.4. Analysis of fringe patterns

The typical fringe pattern of microcrystalline cellulose beam under three-point bending is seen in Fig. 3. This figure also explains the careful selection of bending loads. Higher loads would have formed fringes too close to each other (lack of contrast), and smaller loads would have led to difficulties in the interpretation of bending. A bright fringe is obtained when the phase shift between two overlapping wavefronts was a multiple of 2π. This phase shift is caused by the change in optical path length due to bending, which is twice the vertical displacement at point x on the sample beam (i.e. at any point x of the sample, light has to travel from the original point to the new displaced point; which is the displacement, and back to its original place; i.e. twice the displacement). If the displacement is D_x, then the corresponding phase shift is $(2D_x/\lambda)2\pi$, where λ is the laser wavelength. Furthermore, at the fixed ends of the sample beams (i.e. where there is no displacement), the phase shift is zero, and for the following successive bright fringes 2π, 4π, etc. [9]. Thus, for the nth bright fringe:

Fig. 3. A reconstruction of a double-exposure hologram saved with a CCD camera of a microcrystalline cellulose beam under the three-point bending. The white horizontal line in the middle of the figure is the sample beam, fringe patterns (bright and dark vertical lines) below and above the sample beam describe the bending of the sample beams lower and upper surfaces, respectively, according to Eq. (1).

$$D_x = \frac{n\lambda}{2} \quad (1)$$

Using Eq. (1), the displacement data of the samples can be calculated for the lower and upper surfaces along the sample beam length.

2.5. Evaluation of displacement data

The displacement data, which consisted of data points for the location of the fringe (x) along the reconstructed beam image and the corresponding displacement (D_x), were evaluated separately for the upper

and lower surfaces of the sample beams as tensile and compressive modulus values, respectively. In the cantilever bending method, the moduli could be calculated using a value of maximum displacement (i.e. displacement of the free end of the beam) with the equation of Young's modulus for cantilever bending:

$$E = \frac{4Fl^3}{Dbh^3} \quad (2)$$

where F is the bending force, l length of the beam, D displacement at the free end of the beam, h thickness and b width of the beam. Furthermore, the moduli can also be calculated for all displacement data points along the image of the beam separately using the following equation:

$$E = \frac{2Fl^3}{D_x bh^3}\left[2 - 3\frac{x}{l} + \frac{x^3}{l^3}\right] \quad (3)$$

where D_x is the displacement at point x on the beam. With three-point bending method, the moduli can be calculated using the displacement at the middle point of the beam using Eq. (4):

$$E = \frac{Fl^3}{4D_m bh^3} \quad (4)$$

where D_m is the displacement at the middle point of the beam. Also, along the image of the beam:

$$E = \frac{Fl^3}{4D_x bh^3}\left[3 - \frac{x}{l} - 4\frac{x^3}{l^3}\right], \quad 0 \le x \le 1/2l \quad (5)$$

In four-point bending method, the respective equation of moduli (middle point displacement) is:

$$E = \frac{Fa}{2D_m bh^3}[3l^2 - 4a^2] \quad (6)$$

where a is the gap between the beam support and the place where the bending load is attached. Along the image of the sample beam, Eq. (7) is for the gap between the beam support and the place of the bending load $(0 - a)$, and Eq. (8) for the gap between load attachment points (Fig. 2):

$$E = \frac{2Fx}{D_x bh^3}[3la - 3a^2 - x^2], \quad 0 \le x \le a \quad (7)$$

$$E = \frac{2Fa}{D_x bh^3}[3lx - 3x^2 - a^2], \quad a \le x \le l - a \quad (8)$$

The bending behaviour of the samples was evaluated by visual observation of holographic images as such (i.e. curvature or poor contrast of the fringe pattern at any region of the sample beam hologram), but also calculating the moduli using the whole displacement data obtained from the holographic images. For the calculations, the experimental data points (fringe location and the respective displacement) of each single sample beam were fitted first with the fourth order polynomial equation. According to Eqs. (5), (7) and (8), the ideal bending of the beam should follow a polynomial displacement function. The maximum value of the function was used to calculate the respective moduli values (fitted in Table 1; 3rd column). Secondly, the moduli for every displacement data point of a single sample beam was calculated. For further analysis, both the highest moduli values (max in Table 1) and the mean moduli values (mean in Table 1) were used. Finally, the displacements at the load attachment places (Fig. 2) were used to calculate the respective moduli values (force in Table 1). Furthermore, with the four-point bending method, the middle point moduli values (middle in Table 1) of the sample beams were also obtained. It must be noted that force-values are the middle-point values in the case of three-point bending. After these calculations, the moduli results of single sample beams (five beams with different porosities) were gathered, according to the method for calculating the moduli, and extrapolated to zero porosity using the exponential equation [10]:

$$E = E_0 \exp(-cP) \quad (9)$$

where E_0 is Young's modulus at zero porosity, c is constant and P is sample beam porosity. A comparison of the bending methods and the suitability of moduli calculations was made by evaluating the r^2-values describing the goodness of the fit.

3. Results and discussion

The equations for calculating the moduli were originally established for homogeneous, solid materials such as metals and ceramics. Theoretically, the moduli values obtained for intact specimens should be the same with different bending methods. It could be seen from the results of the bending tests performed, that differences were found in the experimental values of moduli, and the actual bending of the porous sample beams was not ideal (Fig. 4).

With the cantilever bending method, the only meaningful moduli were calculated from the maximum displacement at the free end of the sample beams. This was clearly due to fixing of the other end of the sample beam with the clamp. The pressure holding the sample beam steady induced a stress on the fixed end of the beam resulting in more extensive bending than expected (e.g. more than would have been seen with more ideal metal or ceramic samples). Thus, the calculated moduli values, as a function of the sample beam length, increased clearly from the fixed to the free end (Fig. 4.). Theoretically, the moduli should exhibit a steady line as a function of the sample beam length. Therefore, for soft pharmaceutical materials, it was not possible to calculate moduli values other than the value of maxi-

Table 1
Compressive and tensile modulus values extrapolated to zero porosity using the exponential equation

Material	Bending method	Moduli calculation	Displacement data	E_0	b	r^2
MCC	Cantilever	Max	Compressive	7.27	0.050	0.9463
			Tensile	7.21	0.051	0.9426
	3-Point	Fitted	Compressive	6.17	0.057	0.9633
			Tensile	7.93	0.062	0.9663
		Max	Compressive	6.46	0.058	0.9680
			Tensile	7.81	0.047	0.9311
		Mean	Compressive	5.80	0.061	0.9595
			Tensile	6.62	0.056	0.9456
		Force	Compressive	5.70	0.055	0.9698
			Tensile	7.19	0.059	0.9737
	4-Point	Fitted	Compressive	4.88	0.057	0.9631
			Tensile	6.27	0.062	0.9663
		Max	Compressive	9.58	0.072	0.9994
			Tensile	7.44	0.048	0.9990
		Mean	Compressive	7.33	0.064	0.9984
			Tensile	6.76	0.055	0.9993
		Middle	Compressive	6.95	0.056	0.9996
			Tensile	5.96	0.037	0.9986
		Force	Compressive	7.76	0.060	0.9995
			Tensile	7.03	0.047	0.9996
DCP	Cantilever	Max	Compressive	105.30	0.135	0.9551
			Tensile	102.91	0.134	0.9633
	3-Point	Fitted	Compressive	51.51	0.111	0.9617
			Tensile	39.68	0.092	0.9729
		Max	Compressive	42.10	0.098	0.9500
			Tensile	29.70	0.072	0.9656
		Mean	Compressive	21.94	0.079	0.9665
			Tensile	15.83	0.055	0.9729
		Force	Compressive	51.43	0.109	0.9514
			Tensile	36.94	0.089	0.9635
	4-Point	Fitted	Compressive	52.18	0.101	0.9930
			Tensile	38.36	0.088	0.9971
		Max	Compressive	74.36	0.114	0.9883
			Tensile	43.49	0.091	0.9974
		Mean	Compressive	85.22	0.133	0.9846
			Tensile	43.59	0.107	0.9954
		Middle	Compressive	49.56	0.099	0.9982
			Tensile	49.56	0.099	0.9982
		Force	Compressive	59.13	0.108	0.9903
			Tensile	31.73	0.081	0.9977

MCC is microcrystalline cellulose, DCP is dicalcium phosphate, b is constant in the exponential equation and r^2-value describes the goodness of the fit.

mum displacement. With the three- and four-point bending tests the sample beams were not fixed, only the horizontal movement of the sample beams was restricted. These methods were more suitable for the evaluation of the elasticity of relatively soft pharmaceutical particulate materials.

Unfortunately, α-lactose monohydrate showed significant structural failure as seen in the reconstructed hologram (Fig. 5), where a major curving of the fringe pattern indicates lack of integrity. One corner of the sample beam seemed to be slack indicating lamination of that end of the sample. This type of behaviour was characteristic of nearly all α-lactose samples, thus making it impossible to characterize this material. This type of lack of integrity would not have been noticed, if one would have used conventional displacement detection. This is a good example of the benefits of holographic measurements to determine specimen integrity.

With microcrystalline cellulose, the extrapolated moduli values obtained by the three-point bending showed an unexpected result, with the tensile modulus being slightly higher than the compressive modulus. The difference was clearly noticed in all the moduli calculations. Attachment of bending load to only one particular point in the three-point bending method, instead of to two symmetric places as in the four-point bending method, could result in a less uniformly distributed stress. Thus, the upper surface of the sample

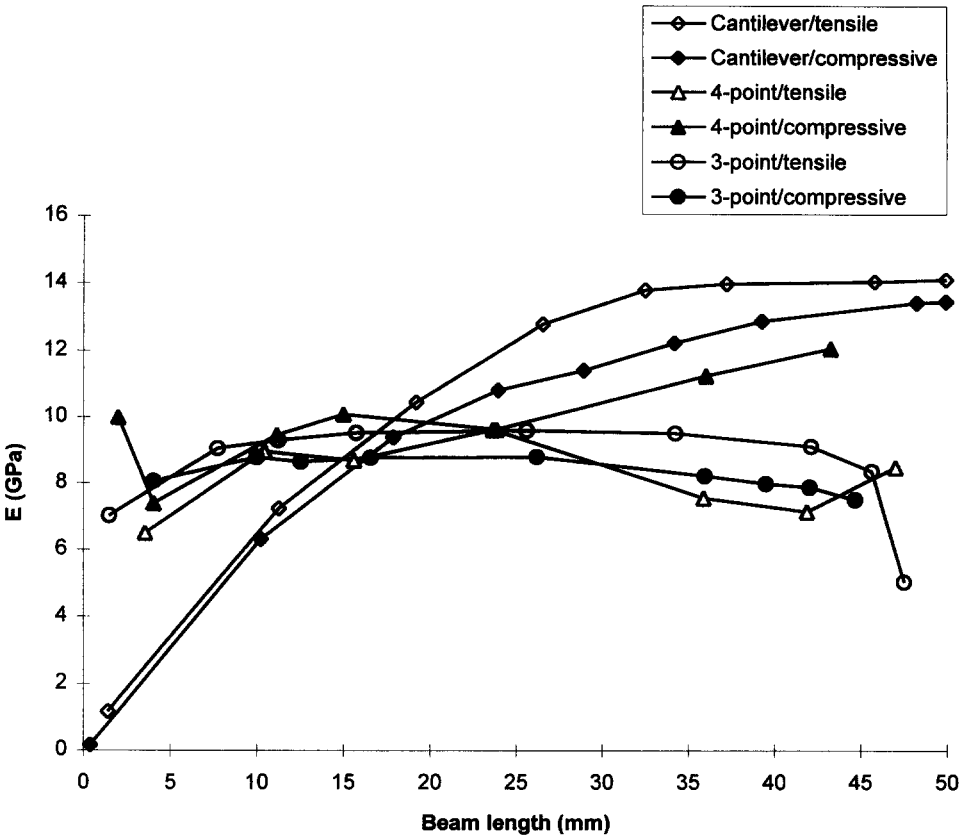

Fig. 4. Calculated moduli as a function of sample beams length (dicalcium phosphate sample beams possessing approximately the same porosity).

beam bent more nearer to the load attachment point. Overall, according to the goodness of fit, (r^2-values; Table 1), the results from the four-point bending fitted better than those from the three-point bending to the exponential equation (Eq. (9)). In most cases, the four-point bending resulted in slightly higher zero porosity moduli values.

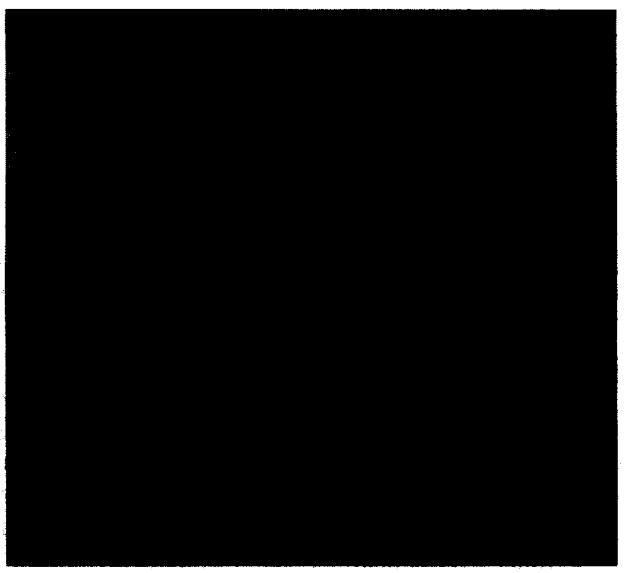

Fig. 5. A reconstruction of a double-exposure hologram saved with a CCD camera of a α-lactose beam under three-point bending. Curving of the fringe pattern of the sample beam upper surface indicates lamination phenomena in the α-lactose sample.

With dicalcium phosphate dihydrate, the values of the compressive modulus were higher than those of the tensile modulus in virtually all cases. Again, the overall goodness of the fit was better and the zero porosity moduli values were slightly higher with the four-point bending method. The cantilever bending method showed considerably higher moduli values when compared to the other methods.

Finally, it can be stated, that the four-point bending results fitted better to the exponential equation than those obtained with the three-point bending method. The attachment of the bending load to two separate places seemed to have a significant effect on the results. At least with the soft pharmaceutical powder compacts, it is important to use a method that ensures the even distribution of the bending stress. If the displacement measurement would have been performed conventionally, i.e. detecting the displacement at the load attachment points, the results would have been in much the same range. This indicates, that the behaviour of the porous beams with three- and four-point bending methods is very similar, however, the four-point bending method leads to a better, more uniform, bending induced distribution of the stress.

Acknowledgements

Sincere thanks are due to Mr Veikko Pehkonen, senior lecturer of mechanics, for his advice concerning the treatment of the bending data.

References

[1] R. Silvennoinen, P. Raatikainen, J. Ketolainen, P. Ketolainen, P. Paronen, Holographic evaluation of bending and integrity of pharmaceutical powder beams, Int. J. Pharm. 131 (1996) 209–217.

[2] F. Bassam, P. York, R.C. Rowe, R.J. Roberts, Young's modulus of powders used as pharmaceutical excipients, Int. J. Pharm. 64 (1990) 55–60.

[3] R.J. Roberts, R.C. Rowe, P. York, The relationship between Young's modulus of elasticity of organic solids and their molecular structure, Powder Technol. 65 (1991) 139–146.

[4] S.K. Dhir, P. Sikora, An improved method for obtaining the general-displacement field from a holographic interferogram, Exp. Mech. 12 (1972) 323–327.

[5] R.J. Pryputniewicz, W.W. Bowley, Techniques of holographic displacement measurement: an experimental comparison, Appl. Opt. 17 (11) (1978) 1748–1756.

[6] R. Silvennoinen, K. Nygrén, M. Mozerov, Holographic nondestructive testing in bone growth disturbance studies, Opt. Eng. 33 (3) (1994) 830–834.

[7] T.Y. Chen, G-L. Chang, S-H. Wu, Holographic evaluation of the marginal fits of complete crowns loaded at the central fossa, Opt. Eng. 34 (5) (1995) 1364–1368.

[8] P. Ridgway Watt, Holographic interferometry in tablet relaxation measurement, J. Pharm. Pharmacol. 33 (1981) 114P.

[9] C.M. Vest. Holographic interferometry, in: S.S. Ballard (Ed.), The Wiley Series in Pure and Applied Optics, Wiley, New York, 1979, pp. 67–77.

[10] R.M. Spriggs, Expression for effect of porosity on elastic modulus of polycrystalline refractory materials, particularly aluminium oxide, J. Am. Ceram. Soc. 44 (1961) 628–629.